ACS NANO

www.acsnano.org

ARTICLE

Reconfiguring DNA Nanotube Architectures *via* Selective Regulation of Terminating Structures

Samuel W. Schaffter,[#] Joanna Schneider,[#] Deepak K. Agrawal, Michael S. Pacella, Eric Rothchild, Terence Murphy, and Rebecca Schulman*

Cite This: https://dx.doi.org/10.1021/acsnano.0c05340

ABSTRACT: **Molecular assemblies inside cells often undergo structural reconfiguration in response to stimuli to alter their function. Adaptive reconfiguration of cytoskeletal networks, for example, enables cellular shape change, movement, and cargo transport and plays a key role in driving complex processes such as division and differentiation. The cellular cytoskeleton is a self-assembling polymer network composed of simple filaments, so reconfiguration often occurs through the rearrangement of its component filaments' connectivities. DNA nanotubes have emerged as promising building blocks for constructing programmable synthetic analogs of cytoskeletal networks. Nucleating seeds can control when and where nanotubes grow, and capping structures can bind nanotube ends to stop growth. Such seeding and capping structures, collectively called termini, can organize nanotubes into larger architectures. However, these structures cannot be selectively activated or inactivated in response to specific stimuli to rearrange nanotube architectures, a key property of cytoskeletal networks. Here, we demonstrate how selective regulation of the binding affinity of DNA nanotube termini for DNA nanotube monomers or nanotube ends can direct the reconfiguration of nanotube architectures. Using DNA hybridization and strand displacement reactions that specifically activate or inactivate four orthogonal nanotube termini, we demonstrate that nanotube architectures can be reconfigured by selective addition or removal of distinct termini. Finally, we show how terminus activation could be a sensitive detector and amplifier of a DNA sequence signal. These results could enable the development of adaptive and multifunctional materials or diagnostic tools.**

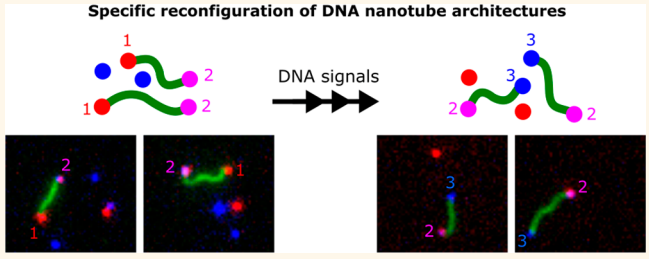

KEYWORDS: *DNA nanotechnology, DNA origami, DNA strand displacement, self-assembly, dynamic nanostructures, nucleic acid diagnostics*

The reconfiguration of self-assembled structures is ubiquitous within living cells. The cellular cytoskeleton, a polymer network composed primarily of actin and microtubule filaments, dynamically assembles and disassembles, and its components rearrange as it adapts to changing environmental cues.[1−3] The adaptive reconfiguration of cytoskeletal networks allows cells to change shape, resist applied forces, and move.[1,3] Reorganization of cytoskeletal filaments that serve as transportation tracks for intracellular cargo also alters when and where materials are delivered within a cell. The cytoskeleton also plays a critical role in determining neuronal structure,[4,5] and adaptive cytoskeletal reconfiguration likely plays an important role in the rearrangement of neuron architectures during development and learning.[6]

The cellular cytoskeleton provides a compelling example of how the adaptive reorganization of a simple polymer network can enable functions within cells that are currently difficult to direct using synthetic materials. Nanotubes self-assembled from carbon,[7,8] inorganic materials,[9] proteins,[10−12] or DNA,[13−15] organized into reconfigurable networks, could enable the construction of adaptive and multifunctional materials with capabilities similar to those of the cellular cytoskeleton. The predictable and programmable sequence specificity of DNA hybridization and largely sequence-independent structure of the DNA double helix makes DNA an attractive material for self-assembling precise nanoscale

Received: June 28, 2020
Accepted: October 6, 2020

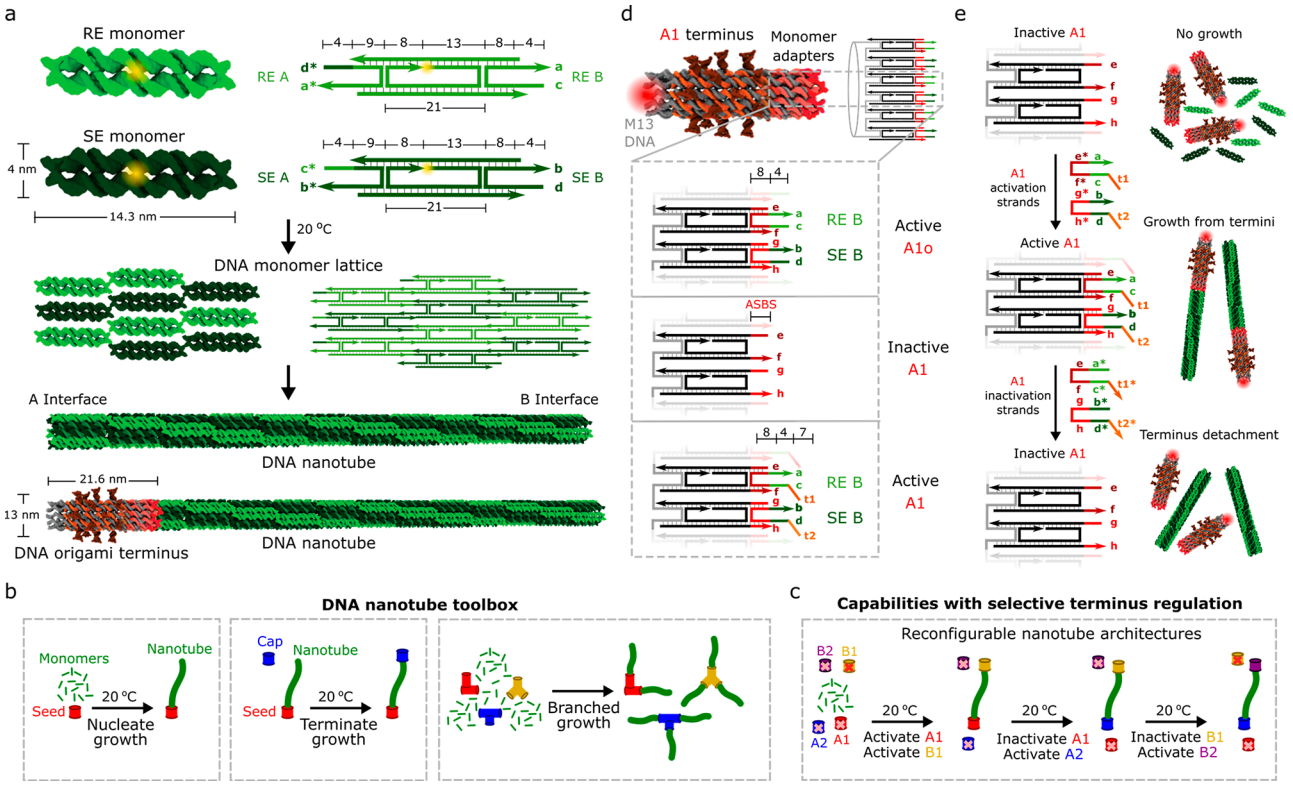

Figure 1. DNA nanotubes and the design of a nanotube terminus whose binding activity for DNA nanotubes can be specifically activated and inactivated. (a) DNA nanotube monomers and DNA nanotube structure. Top: DNA monomers are DAE-E double crossover molecules[35] that self-assemble from five strands of synthetic DNA. Monomers consist of two DNA helices that are rigidly bound by two crossover motifs with four single-stranded sticky end regions on the two helix ends (a, b, c, and d with complementary sequences denoted by *). Each of the two types of monomers that co-assemble to form the nanotube has both an A interface and a B interface, each defined by the sticky end sequences on each side of the monomer. Each monomer contains a Cy3 fluorophore (yellow) at the 5′ end of its central strand. Numbers labeling monomer domains indicate domain lengths in bases. Middle: Complementary sticky ends program lattice architecture. Bottom: A cyclized lattice forms a nanotube.[15] Each nanotube has an A interface and a B interface defined by the free sticky ends at each nanotube end. DNA nanotube growth can be nucleated at a DNA origami terminus. (b) DNA nanotube toolbox. Left: DNA origami seeds can nucleate nanotube growth.[14] Middle: Capping structures that bind to nanotube ends can terminate nanotube growth.[24] Right: Branched DNA origami seeds can be used to grow nanotubes at specific angles relative to one another.[23] (c) Schematic of nanotube architecture reconfiguration by successive activation and inactivation of orthogonal termini that interact with a specific interface of the monomers/nanotubes. Red Xs represent inactive termini. Similar reconfigurations could be achieved with branched termini. (d) A DNA origami terminus is a hollow cylinder consisting of an M13 DNA scaffold folded by staple strands. Unfolded portions of the M13 serve as docking sites for fluorescently modified oligos (typically atto488 is used, see Supplementary Section 1.2 and Supplementary Table S21). The terminus nucleates DNA nanotube growth at monomer adapter structures that form a facet onto which DNA monomers can attach. There are six monomer attachment sites around the circumference of the terminus. An active A terminus binds to the A interface of the monomers and/or nanotubes (top and bottom panels). An inactive terminus is missing the adapter strands that bind to the monomer sticky ends, so no nanotube nucleation can occur on them (middle panel). Termini that can be inactivated have adapter strands that each have a 5′ single-stranded region on the sticky end strands that serves as a toehold in a toehold-mediated strand displacement reaction that removes the sticky end strands. (e) Schematic of sequential terminus activation and inactivation.

structures,[16−19] including DNA nanotubes,[13−15,20−22] which can be organized hierarchically.[23−26] Further, programmable DNA strand displacement reactions enable dynamic rearrangement of such DNA nanostructures.[27−29]

Here, we study DNA nanotubes consisting of monomers composed of five DNA strands that self-assemble into nanotubes *via* hybridization of single-stranded sticky ends (Figure 1a). These DNA nanotubes can serve as scaffolds for precise arrangement of other materials, allowing their structure to template a range of functions.[30−34] Specific control over when and where nanotubes grow, how nanotubes are arranged relative to one another, and nanotube length could make it possible to build complex DNA nanotube networks. Control over when and where nanotubes grow as well as nanotube orientation has been achieved using scaffolded DNA origami seeds that serve as nucleation sites by mimicking a nanotube growth face[14,23] (Figure 1b, left). Other DNA structures can cap the growing ends of nanotubes, terminating their growth and controlling the lengths nanotubes reach[24] (Figure 1b, middle). Assembly processes that integrate DNA nanotube monomers, seeds, and/or caps can form specific types of simple networks, including those that self-assemble to connect specific anchored seeds on a surface[26] or branched seed structures in which there are specific programmed angles between nanotubes[23] (Figure 1b, right). These nanotube architectures could serve as building blocks for larger, complex networks. However, there is currently no mechanism to rearrange these nanotube architectures in response to environmental stimuli.

https://dx.doi.org/10.1021/acsnano.0c05340
ACS Nano XXXX, XXX, XXX−XXX

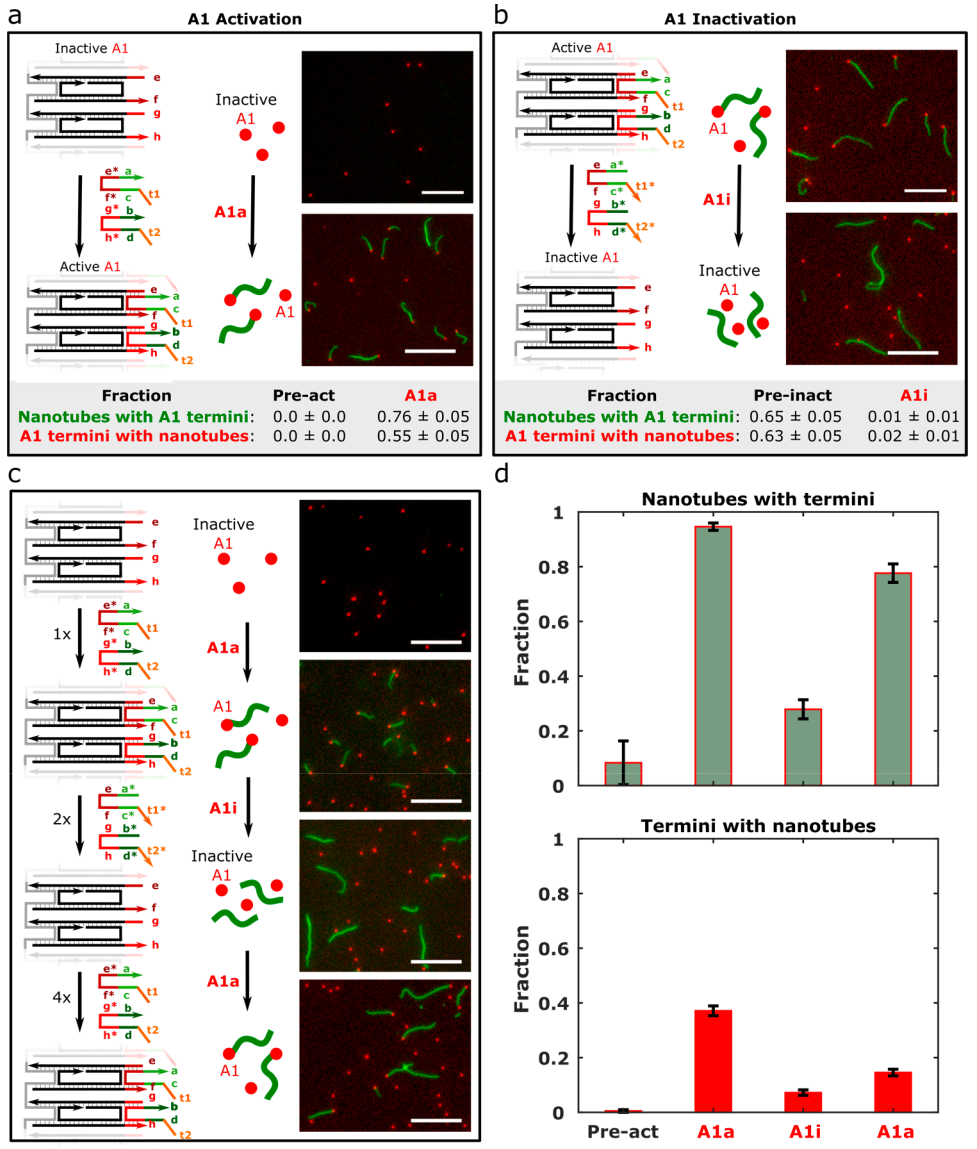

Figure 2. DNA nanotube termini can be activated and inactivated by specific DNA sequence inputs. (a, b) Schematics of terminus activation (a) and terminus inactivation (b) with representative fluorescence micrographs of results. To characterize activation, inactive termini were first incubated with monomers (pre-act), and activation strands (A1a) were then added. To characterize inactivation, active termini were incubated with monomers to facilitate nanotube growth (pre-inact), and then inactivation strands (A1i) were added. The fractions of nanotubes with termini and termini with nanotubes are tabulated below. (c) Schematic of an experiment during which termini are sequentially activated, inactivated, and then reactivated *via* successive additions, respectively, of activation, inactivation, and activation strands. Representative fluorescence micrographs of results are shown for each stage of reconfiguration. 1×, 2×, and 4× refer to the ratio of the concentrations of the activation or inactivation strands added for a given reconfiguration step, relative to the concentration of A1a added to direct the first terminus activation. (d) Fractions of nanotubes with termini and termini with nanotubes for the experiment in (c). The small fraction of nanotubes attached to termini before activation is likely; the result of homogeneous nucleation followed by nonspecific binding of these nanotubes to termini.[24] See Supporting Information Table S12 for further experimental details. Error bars represent 95% confidence intervals of proportions. Scale bars: 10 μm.

Here, we demonstrate how such specific reorganization of DNA nanotube architectures can be achieved. We develop the capacity for programmable reconfiguration of nanotube architectures by selectively regulating the binding activity of different DNA origami structures, which we term DNA origami termini, to DNA monomers or nanotube ends (Figure 1c). We design DNA hybridization and strand displacement reactions that can specifically activate or inactivate DNA origami termini. We demonstrate how different termini can be specifically attached and detached from nanotubes using selective activation and inactivation of the termini's ability to bind nanotube ends. Using four orthogonal termini, we show how nanotube architectures attached to termini on both ends can be selectively reconfigured *via* specific activation and inactivation of different termini in succession. Our approach thus enables micron-scale structural rearrangements to be achieved through regulation of the binding affinity of a few nanoscale junctions. These results thus introduce an efficient means for dynamically rearranging DNA nanotube architectures that could enable the development of reconfigurable multifunctional nanotube structures, controlled self-assembly

https://dx.doi.org/10.1021/acsnano.0c05340
ACS Nano XXXX, XXX, XXX−XXX

of hierarchical nanotube networks, or, through signal amplification *via* terminus activation, sensitive diagnostic tools.

RESULTS AND DISCUSSION

Design of DNA Origami Termini That Can Be Activated and Inactivated. We sought to develop a means to reconfigure DNA nanotube architectures by using specific DNA sequences to trigger specific reconfiguration operations. We began by designing a mechanism to use distinct DNA sequences to specifically activate and inactivate a DNA origami structure that has been used as both a seed for nucleating nanotube growth[14] and a cap for terminating growth.[24] We termed such a structure a DNA origami terminus, since it can serve as either a nanotube seed or cap and is attached to the end of a nanotube (Figure 1b). A DNA origami terminus interacts with DNA monomers or nanotubes *via* monomer adapter structures. There are six adapter structures around the interface of a terminus that each present monomer sticky end sequences; together these structures mimic the structure of a nanotube growth facet. There are three adapter structures that present RE sticky ends and three adapter structures that present SE sticky ends (Figure 1d, top panel). For the terminus shown in Figure 1b, which we term an A1 terminus, the adapter structures present the sticky end sequences that allow them to bind to the A interface of the monomers to nucleate growth[14,26] or join with the A interface of DNA nanotubes to terminate growth.[24] We created a method to control terminus activity in which inactive termini are missing the strands that present the sticky end sequences on all six of the adapter structures, meaning that the terminus cannot interact with monomers or nanotubes (Figure 1d, middle panel). This inactive terminus is activated by adding the adapter sticky end strands (called the activation strands) that specifically bind to the interface of the inactive terminus (Figure 1e). The activation strand binding sites (ASBS in Figure 1d, middle panel) on the adapter structures that bind the RE activation strands were designed to each have the same sequence, and the ASBS of the SE activation strands likewise have the same sequences. As a result, only two sequences are required to activate a terminus.

Inactivating a terminus that is bound to the end of a DNA nanotube in our design involves removing the adapter sticky end strands from the bound terminus. To facilitate these strands' removal, we designed the activation strands to include 7-base single-stranded domains at their 5′ ends (Figure 1d, bottom panel). These single-stranded domains facilitate a toehold-mediated DNA strand displacement[36] reaction where strands complementary to the activation strands bind to the activation strands on a terminus and removes them. This removal inactivates the terminus and, if the terminus is bound to a DNA nanotube, removes the terminus from the nanotube end (Figure 1e).

Activation Strands Trigger Nanotube Growth from Termini and Inactivation Strands Remove Termini from Nanotubes. We first tested whether inactive DNA origami termini would not nucleate nanotube growth until their designed activation strands were added. We incubated inactive A1 termini with 45 nM DNA monomers at 20 °C, conditions at which nanotubes could grow from termini but only rarely nucleated homogeneously.[24] No termini nucleated nanotube growth (N = 91) after 6 or 24 h of incubation (Figure 2a and Supporting Information Figure S1, respectively), and 5-fold fewer nanotubes were observed than when the same concentration of active termini was incubated with monomers (Supporting Information Figure S1). We next tested terminus activation by adding the A1 adapter sticky end strands (activation strands) to inactive A1 termini after a 6 h incubation with 45 nM monomers. We used 50 nM of the activation strand, a typical concentration of the output of a DNA strand displacement circuit with the idea that such an activation process might be directed or regulated by upstream circuits.[27] Twenty-one h after the addition of the activation strands, nearly 50% of the termini had nucleated nanotube growth and nearly 80% of nanotubes that had grown were attached to termini (Figure 2a). This measured yield of A1 activation varied somewhat (40−65%) across experiments as well as time points (see Materials and Methods). Similar fractions of activated termini with nanotubes and of nanotubes attached to termini were observed when using activation strands with and without the 7-base single-stranded toehold domains (Figure 2a and Supporting Information Figure S2a), indicating that the toeholds do not significantly affect the process of nanotube nucleation from an active terminus. Given that only 50−60% of termini annealed in an active form nucleated nanotubes (Figure 2b and Supporting Information Figure S1), a 50% yield of active termini after the addition of the activation strands indicates that activation recovers over 80% of terminus activity. The yield of nanotube growth from termini could likely be improved by using gel-purified adapter and activation strands, as a significant fraction of the unpurified strands that are used have defective adapter structures (which raises the barrier to nucleation from these structures). It would also be expected that the yield of nanotube growth is influenced by the concentrations of termini and monomers used. The small energy barrier to nucleation from termini means that nucleation from termini stops when the monomers are depleted below a certain threshold, but growth from existing nanotubes is still possible.[14]

We next investigated whether the termini could be removed from the nanotubes after growth by adding inactivation strands (Figure 1e). We annealed termini with the A1a strands, incubated these active termini with 45 nM monomers to nucleate nanotube growth, and after 22 h of growth, added inactivation strands complementary to the A1a strands (A1i). As expected, nearly all of the termini with the 5′ toehold domains detached from the nanotubes (<2% of termini still attached) upon addition of the inactivation strands (Figure 2b). No detachment of termini whose activation strands lacked the single-stranded 5′ domains was observed (Supporting Information Figure S2b). Termini can therefore be reliably inactivated following the designed pathway of toehold-mediated strand displacement of the activation strands from the termini.

Sequential Activation and Inactivation of Termini. A reconfigurable nanotube architecture might be expected to take on many different morphologies over time, involving multiple steps of activation and inactivation of specific termini depending on the reconfiguration pathway. We thus next investigated whether terminus activation and inactivation could be orchestrated multiple times in succession by adding activation and inactivation strands sequentially. We first tested inactivation followed by activation by growing nanotubes from active A1 termini, adding inactivation strands (A1i) and after terminus inactivation, adding activation strands (A1a). We found 80% of the termini were removed from the nanotubes within 4 h of the addition of the inactivation strands and over

https://dx.doi.org/10.1021/acsnano.0c05340
ACS Nano XXXX, XXX, XXX−XXX

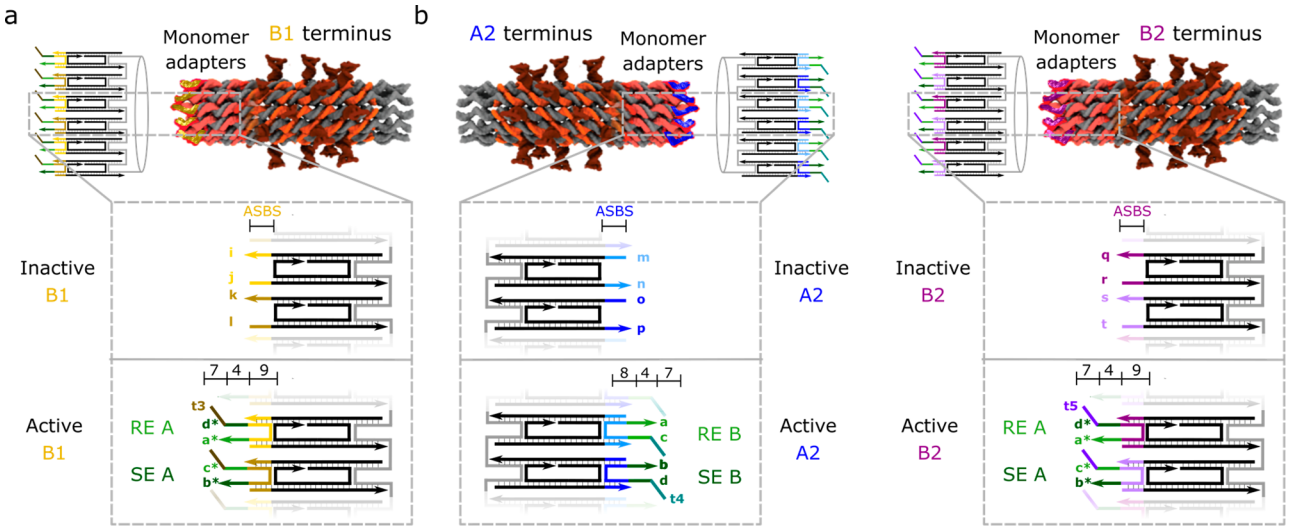

Figure 3. Designs of additional termini activated and inactivated by orthogonal sets of activation and inactivation strands. (a) The B1 terminus binds to the B interface of monomers and nanotubes. (b) A2 and B2 termini that bind the A or B interfaces of monomers and nanotubes, respectively. Each terminus has distinct activation strand binding sites (ASBS) and distinct toehold domains on its activation strands. Numbers indicate domain lengths in bases. Letters indicate domain sequence identity with * denoting complementarity. Sequences in Supporting Information Sections 1.3 and 1.4.

80% of the nanotubes in solution were attached to termini after the reactivation step (Supporting Information Figure S3). Inactive A1 termini could also be mixed with monomers, activated to grow nanotubes (resulting in >95% nanotubes with termini), then inactivated (leaving <30% nanotubes with termini), and finally reactivated (reattaching roughly 80% of nanotubes to the termini) (Figure 2c,d). To ensure that each activation or inactivation step removed all of the activation or inactivation strands from the previous step, we increased the concentration of the strands added at each step (Figure 2c).

When measured as the fraction of nanotubes attached to termini, reactivation appears to proceed almost to completion. However, the fraction of termini with nanotubes on them is 30% lower after the second activation step than after the first (Figure 2d). After terminus inactivation, when both the A and B interfaces of the nanotubes are free, end-to-end joining of nanotubes[26,37] may reduce the number of nanotubes in a sample (*i.e.*, the concentration of nanotube ends). Since the concentration of the termini does not change, end-to-end joining would decrease the maximum yield of termini with attached nanotubes that could be achieved (Supporting Information Figure S4).

Design of Orthogonal DNA Origami Termini That Can Be Selectively Activated and Inactivated. The ability to activate/inactivate specific DNA origami termini that bind to different nanotube binding interfaces would make it possible to build and reconfigure more complex nanotube architectures (Figure 1c). To demonstrate how multiple structures could be attached and detached from each of the two ends of a nanotube, we first designed a terminus that could bind to the B interface of the DNA monomers or nanotubes, that is, on the opposite side of the DNA nanotubes from where the A1 terminus binds (the B1 terminus in Figure 3a). To prevent binding crosstalk during activation or inactivation of the A1 or B1 termini, we designed the sequences for the ASBS on the adapter structures of the B1 terminus to be distinct from those used for the ASBS of the A1 terminus (Figure 3a). We also designed a second A terminus (A2) and a second B terminus (B2), each with their own distinct ASBS sequences, and thus their own activation and inactivation strands (Figure 3b). After activation and inactivation of each of these individual termini in isolation (B1, A2, or B2), >75% of nanotubes were attached to termini after activation, and <20% of nanotubes were attached to termini after inactivation. We also observed, as in previous studies,[24] that the two B termini had lower nucleation yields (fraction of termini with nanotubes) than the two A termini (Supporting Information Section 4).

A1 and B1 Termini Can Be Specifically Activated and Inactivated to Assemble and Disassemble Doubly Terminated Nanotube Architectures. To demonstrate how successive activation and inactivation of different termini could alter a nanotube architecture, we used these steps to assemble and disassemble a simple nanotube architecture: a nanotube attached to a terminus at each of its two ends, termed a doubly terminated architecture.[24] We first investigated whether the A1 and B1 termini could be sequentially activated to assemble a doubly terminated nanotube architecture and subsequently inactivated to disassemble this nanotube architecture (Figure 1c, left). We combined inactive A1 and B1 termini with monomers, then added A1a strands to initiate growth from the A1 termini. After 5 h, almost 90% of the nanotubes that grew were attached to A1 termini and fewer than 5% were attached to B1 termini, indicating selective A1 activation (Figure 4). We then added the B1 activation strands and after a 13 h incubation and found that roughly 70% of the nanotubes were attached to B1 termini and 67% of nanotubes attached to B1 termini were also attached to A1 termini (Supporting Information Table S22). Doubly terminated A1−B1 architectures can form by either an activated B1 terminus binding to a nanotube with an A1 terminus attached at its opposite end or an activated B1 terminus nucleating growth and then joining end-to-end[26,37] with a nanotube attached to an A1 terminus. Given that when B1 termini are mixed with monomers, the activation of the B1 terminus resulted in <20% nucleation yield (Supporting Information Figure S5), the majority A1−B1 terminated architectures likely formed because B1 termini bound to the ends of existing nanotubes. While 67% of the nanotubes attached to B1 termini were

https://dx.doi.org/10.1021/acsnano.0c05340
ACS Nano XXXX, XXX, XXX−XXX

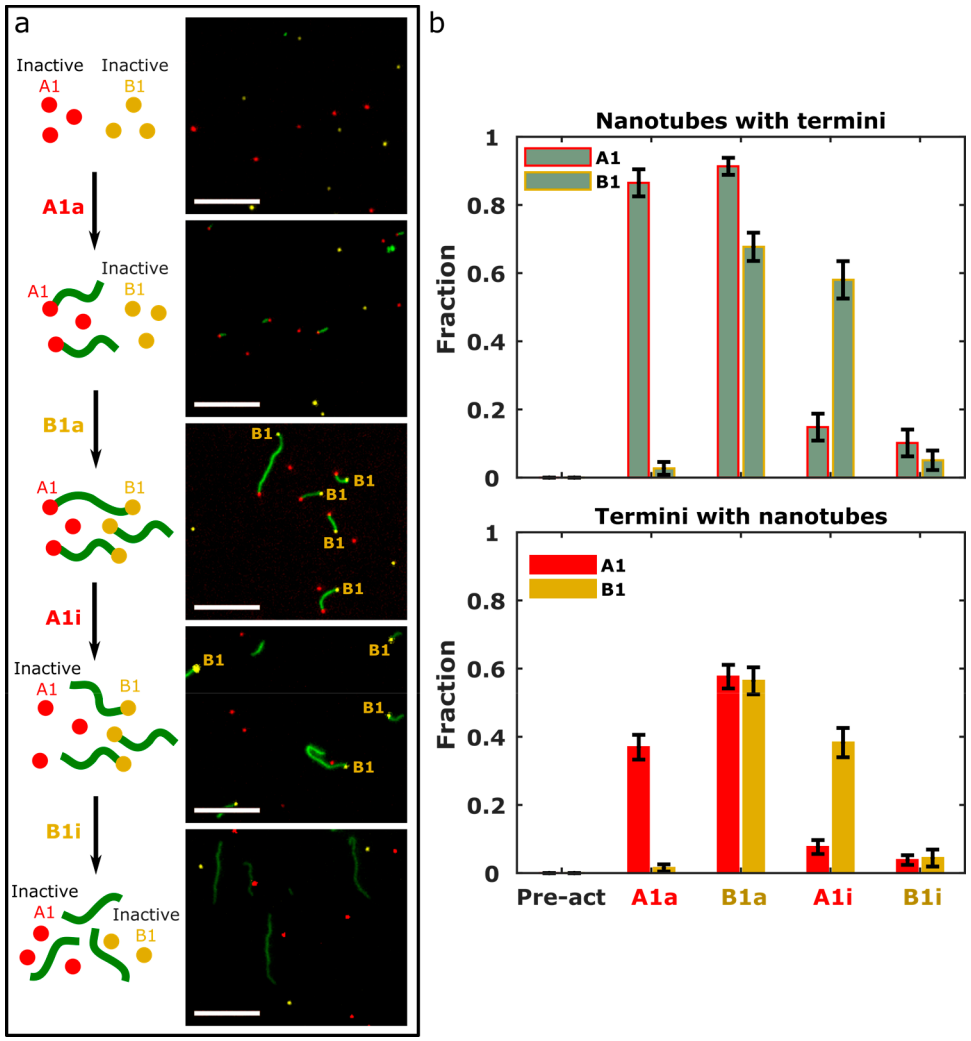

Figure 4. Doubly terminated nanotube architectures can be assembled and disassembled by selective activation and removal of individual termini. (a) Schematic of an experiment testing the efficacy of sequential activation and inactivation of A1 and B1 termini along with representative fluorescence micrographs of results after each activation or inactivation step. For clarity, all B1 termini attached to nanotubes are labeled. (b) Fractions of nanotubes with termini and termini with nanotubes during each of the steps of the experiment in (a). The yields of doubly terminated A1−B1 architectures (Supporting Information Section 6.3) are tabulated in Supporting Information Table S22. See Supporting Information Table S13 for further experimental details. Error bars represent 95% confidence intervals of proportions. Scale bars: 10 μm.

incorporated into A1−B1 terminated architectures, only 50% of nanotubes attached to A1 termini were also attached to B1 termini (Supporting Information Table S22). If each termini's activation efficiency is 50−60%, we might expect that only half of the nanotubes attached to A1 termini would also become attached to B1 termini. Sequential addition of A1 and then B1 inactivation strands successively removed termini from both nanotube ends, leaving no nanotubes with both termini still attached (N = 59) (Supporting Information Table S22). These results demonstrate that the A1 and B1 activation/inactivation strands can selectively control the activity of their DNA origami targets and that doubly terminated nanotube architectures can be selectively assembled and disassembled. We were also able to selectively assemble an A1−B1 doubly terminated structure and then successively remove and reattach the A1 terminus with similar yields (Supporting Information Figure S8) to the results in Figure 4, demonstrating how doubly terminated structures can be dynamically formed, disassembled, and reformed.

Doubly Terminated Nanotube Architectures Can Be Reconfigured *via* Selective Terminus Activation and Inactivation. We next sought to use terminus activation and inactivation to reconfigure a doubly terminated nanotube architecture by changing what terminating structures were attached to the nanotubes' ends. As doubly terminated structures can link two termini bound to surfaces or other objects,[26] switching which termini are attached could be used to change the surfaces or objects that a nanotube links. We devised an experiment to first assemble an A1−B2 terminated nanotube architecture and then construct A2−B2 terminated architectures using the nanotubes that initially connected the A1 and B2 termini. We started the experiment by combining inactive A1, B2, and A2 termini with monomers. We then added the A1 activation strands (A1a) to initiate growth from the A1 termini. After 19 h, 80% of the nanotubes that grew were attached to A1 termini and fewer than 15% were attached to either an A2 or B2 terminus (Figure 4), demonstrating the specificity of A1 activation. We then added B2 activation

https://dx.doi.org/10.1021/acsnano.0c05340
ACS Nano XXXX, XXX, XXX−XXX

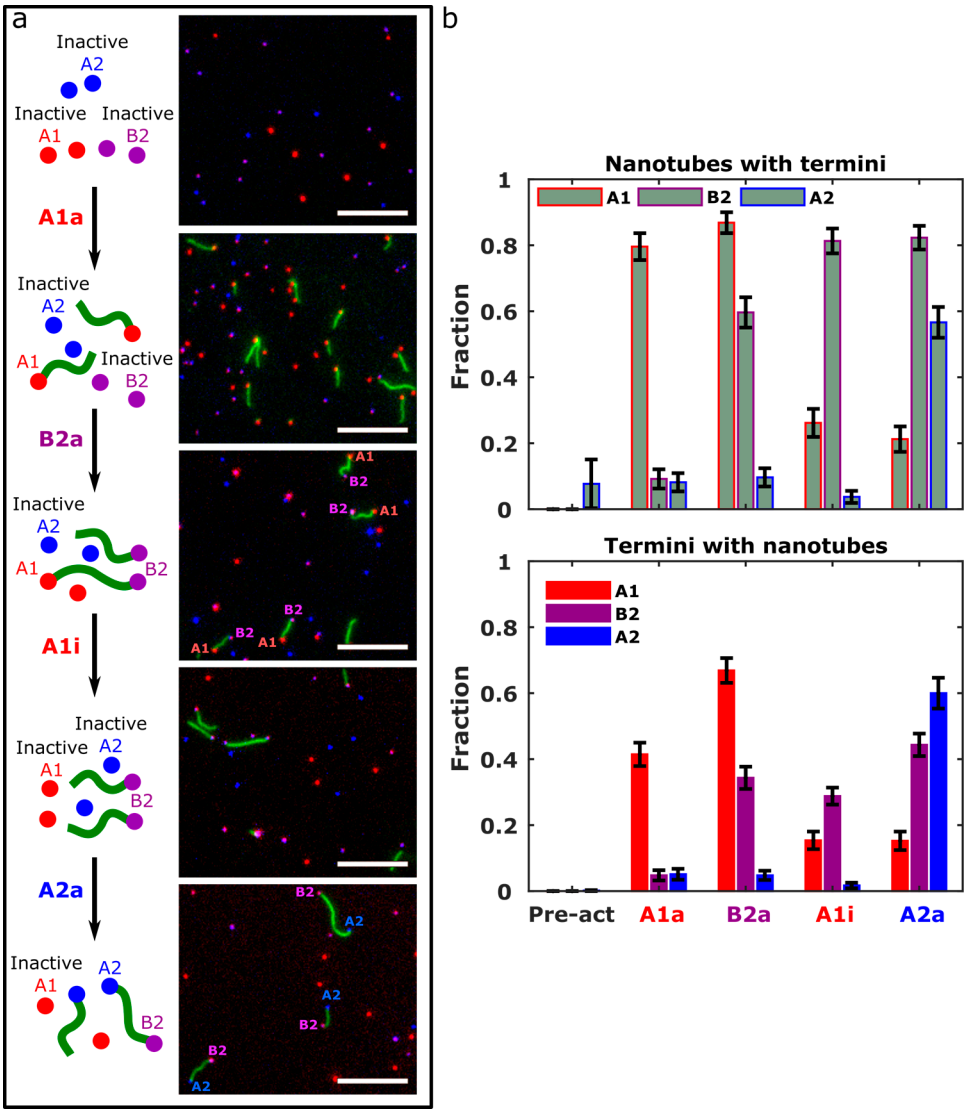

Figure 5. Selective reconfiguration of doubly terminated nanotube architectures. (a) Schematic of an experiment demonstrating the stepwise transformation of an A1−B2 terminated structure to an B2−A2 terminated structure *via* selective terminus activation and inactivation and fluorescence micrographs showing example results. Termini on the doubly terminated structures in the micrographs are labeled for clarity. (b) Fractions of nanotubes with termini and termini with nanotubes for the experiment in (a). Each stage of the experiment is initiated with the addition of the activation or inactivation strands in the respective *x*-axis label. The yields of doubly terminated A1−B1 architectures (Supporting Information Section 6.3) are tabulated in Supporting Information Table S24. The small fraction of nanotubes attached to termini before activation in is likely the result of homogeneous nucleation followed by nonspecific binding of these nanotubes to termini.[24] See Supporting Information Table S14 for further experimental details. Error bars represent 95% confidence intervals of proportions. Scale bars: 10 μm.

strands (B2a) to form A1−B2 terminated nanotube architectures. After 6 h, consistent with the results presented in Figure 4, the majority (85.3%) of nanotubes attached to a B2 terminus were also attached to an A1 terminus (Supporting Information Table S24). Additionally, the percentage of nanotubes attached to A2 termini still remained lower than 15% (Figure 5), demonstrating specific B2 activation. To reconfigure the A1−B2 terminated structure to produce an A2−B2 terminated structure, we next added the A1 inactivation strands (A1i) which detached the A1 termini from nanotubes, reducing the percentage of nanotubes A1-B2 doubly terminated architecture to under 20% in 3.5 h (Supporting Information Table S24). Finally, we added the A2 activation strands (A2a) to form A2−B2 terminated nanotube architectures. After 24 h, 75% of the nanotubes attached to A2 termini were also attached to a B2 termini and thus were parts of A2−B2 terminated structures (Supporting Information Table S24). These results demonstrate that nanotube architectures can be reconfigured by selectively regulating the activity of a library of DNA origami termini in a stepwise fashion.

Terminus Inactivation for Stepwise Assembly of Hierarchical Nanostructures. We next asked whether we could apply terminus activation/inactivation to the problem of hierarchical assembly of branching nanostructures. We have previously demonstrated[23] that multi-armed DNA nanotube structures with specific geometries may be nucleated from DNA origami seeds with multiple adapter interfaces presented at specific angles. These structures offer the possibility of constructing branching dendritic nanotube structures akin to

https://dx.doi.org/10.1021/acsnano.0c05340
ACS Nano XXXX, XXX, XXX−XXX

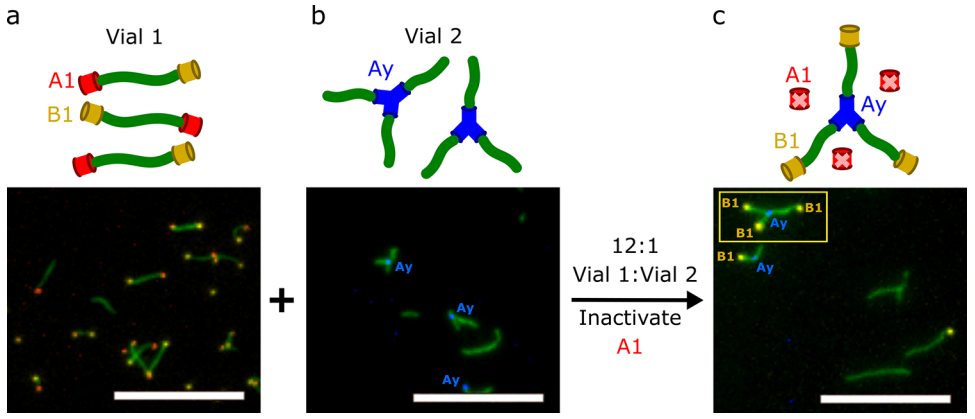

Figure 6. Stepwise assembly of hierarchical nanostructures *via* terminus inactivation. (a) "Y" DNA nanotube structures grown from Y-shaped DNA origami termini an A interface on all three arms (Ay). (b) A1−B1 doubly terminated nanotubes grown from A1 termini and capped with B1 termini. (c) The doubly terminated nanotubes in vial 1 were mixed in a 12:1 ratio with the Y nanotube structures in vial 2, and the A1 termini were inactivated to allow end-to-end joining between B1 terminated nanotubes and Y nanotube structures. The yellow box encloses an example target structure where a Y nanotube architecture has joined to a B1 terminated nanotube on all three arms. A2 and B1 termini are labeled in micrographs for clarity. See Supporting Information Table S15 for further experimental details. Scale bars: 10 μm.

cytoskeleton growth.[4] However, a key feature of cytoskeletal networks is the ability to dynamically rearrange and either expand or contract depending on cellular conditions. Terminus activation/inactivation provides an ideal mechanism for mimicking this kind of behavior.

As a proof of concept, we studied a simplified process of this activation and inactivation: the end-to-end joining of a population of three-armed "Y" nanotube structures nucleated from Y-shaped DNA origami termini[23] presenting the A interface with a population of one-dimensional nanotube structures. The one-dimensional nanotube structures were first grown from A1 seeds over 20 h and then terminated *via* the addition of B1 termini (Figure 6a). The resulting structures were then mixed in 12-fold excess with pregrown Y nanotube structures (Figure 6b). The A1−B1 doubly terminated nanotubes were protected from joining to the Y nanotube structures. To deprotect the A1−B1 terminated structures, we inactivated the A1 termini which allowed joining of the nanotubes to the Y structures (Figure 6c). In principle, the procedure outlined above could be used to stepwise assemble branching DNA nanotube architectures.

Terminus Activation for Sensitive Nucleic Acid Sequence Detection. The above results demonstrate that terminus activation and inactivation can be used to sequentially build and reorganize DNA nanotube architectures. Reorganizing an architecture by the activation and inactivation of termini is an efficient means of achieving large-scale structural change or the initiation of a nanotube assembly process in response to only a small concentration of an input signal because there are typically over 1000-fold more monomers (present in our experiments at 45 nM) than termini (present in our experiments at approximately 3 pM).

In principle, because only a few strands of DNA are required to activate (or inactivate) a terminus, and termini are present at picomolar concentrations, picomolar concentrations of activator strand should be able to trigger seed activation and thus assembly of nanotubes. Thus, we next sought to investigate whether terminus activation could be adopted to sensitively detect a specific DNA sequence. We focused on the case where the response of the system is the assembly of DNA nanotubes, that is, the formation of fluorescent structures many micrometers in length. Initiation of DNA nanotube self-assembly in response to specific chemical signals (both nucleic acids and proteins) has previously been explored[38,39] and proposed as a potential tool for point-of-care diagnostics.[39] In these previous demonstrations, input signals converted inactive monomers into active monomers that then spontaneously self-assembled into nanotubes for detection. This input signal required concentrations on the order of 100 nM to activate enough monomers for growth. Our termini activation scheme could potentially be much more sensitive as we only need to activate 1−5 pM of termini to initiate seeded growth. Related methods for detecting long single-stranded DNA strands use this type of amplification and are executed by annealing the sample with staples that fold the long single-stranded DNA into a nucleation sites for DNA nanostructure self-assembly.[40] Here we sought to detect short single-stranded sequences *in situ* at room temperature by using these strands to complete a mostly folded, but inactive nucleation site.

To investigate the sensitivity of terminus activation in response to sequence inputs, we added 0.1, 1, 10, and 100 nM of the activation strands to respective solutions of 3 pM inactive A1 termini and 45 nM nanotube monomers. In theory, based on the stoichiometry, activation should complete when just 9−10 pM of these strands are added. However, surprisingly, fewer than 2% of termini were activated when 1 nM of the activation strands were added (almost a 100-fold excess of activation strands with respect to their binding sites), and no detectable nucleation was observed with 0.1 nM of activation strands (Figure 7a).

We thus asked why high concentrations of activation strands were necessary. We found that the sequences of the activation strands, which were previously designed to assemble into adapter structures during annealing,[24,26] were actually predicted to have significant secondary structure and thus could fold on themselves rather than attach to the ASBS of termini in our isothermal activation experiments at 20 °C (Supporting Information Figure S9). To investigate whether the presence of this secondary structure was a factor in the high concentration of activation strands needed for terminus activation, we designed another terminus (A3) with activation strands that are predicted to have no significant secondary structure at 20 °C (Supporting Information Section 5). When 1 nM of these activation strands was added to 3 pM of inactive

https://dx.doi.org/10.1021/acsnano.0c05340
ACS Nano XXXX, XXX, XXX−XXX

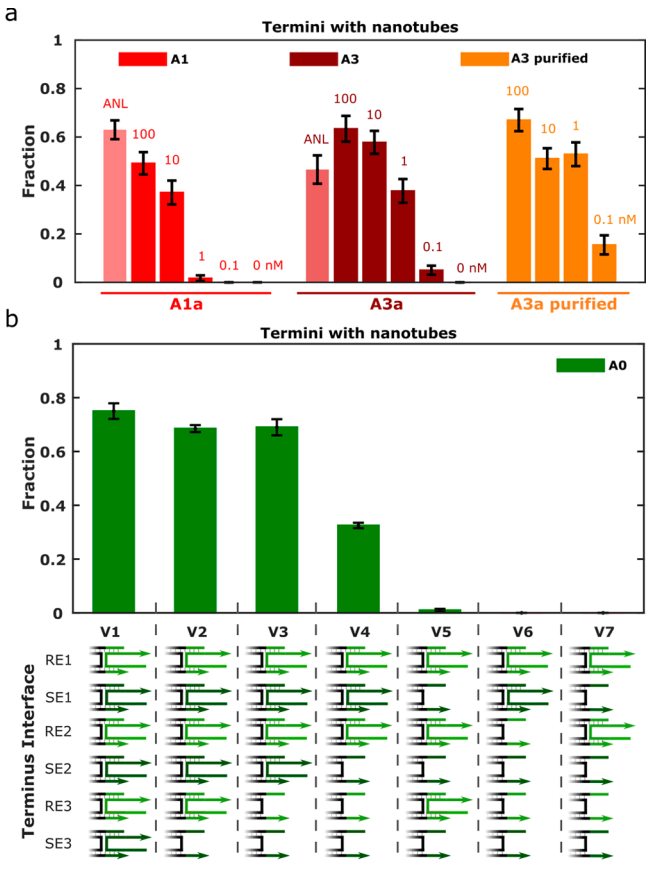

Figure 7. Sensitive detection of activation sequences and activation using a single activator strand sequence. (a) Fractions of termini with nanotubes after activation of the A1 terminus (A1a) or A3 terminus using unpurified (A3a) or PAGE purified activation strands (A3a purified) from IDT. The activation strands were added to the final concentrations (nM) listed above the bars as soon as the purified termini were added to the monomer mixes. The "ANL" (annealed) samples served as positive controls: These termini were annealed with their activation strands. The samples were analyzed 24 h after the activation strands were added. Termini were at 3 pM in all samples. All termini were fluorescently labeled with atto488. Error bars represent 95% confidence intervals of proportions. (b) Fraction of termini with nanotubes from terminus variants with different sets of presented activation strands after 25 h of growth. The A0 terminus used six distinct ASBS sequences to make it possible to prepare terminus variants with arbitrary combinations of sticky ends for nanotube binding. The A0 terminus did not possess the 7-base 5′ single-stranded toeholds that are used during inactivation but not during activation. The A0 terminus variants were each present at 25 pM. Monomer concentration was 45 nM. Essentially, no nucleation occurs from variant V5, where all the SE sticky ends are missing, suggesting that this variant could be used as an inactive terminus that could be activated by the addition of a single SE activation sequence. All A0 terminus variants were present at roughly 25 pM. All A0 variants were fluorescently labeled with atto647.

A3 termini and 45 nM monomers, roughly 40% of the A3 termini grew nanotubes, many more than the <2% of A1 termini when 1 nM of A1 activation strands was added to these termini under the same conditions (Figure 7a and Supporting Information Figure S10). Yet hardly any A3 activation (<5%) was observed when only 0.1 nM of the activation strands was used. We theorized that this might be because we used unpurified activation strands of which a significant fraction (according to IDT, which synthesized the strands, as many as 30−40% of strands may have sequence errors). To test whether these sequence errors limited activation, we used 0.1 nM of PAGE purified A3 activation strands to 3 pM inactive A3 termini and 45 nM monomers. After 24 h of incubation, nearly 20% of A3 termini grew nanotubes (Figure 7a and Supporting Information Figure S10). Further, the fraction of A3 termini that grew nanotubes after 0.1 nM of purified strands was added increased to nearly 40% after a longer incubation period (Supporting Information Figure S10). Thus, using PAGE purified activation strands can further enhance activation sensitivity down to the subnanomolar range. In these experiments, the adapter strands (other than the activation strands) were not gel purified; activation of nanostructures assembled using purified adapter strands, which have fewer sequence errors, might further increase the sensitivity of this process.

We next asked whether we could modify the terminus activation scheme such that just a single nucleic acid sequence could be used for activation. In our previous experiments, we designed inactive termini that were activated by adding all six adapter sticky end strands and required two distinct sequences for activation (one for the RE adapters and one for the SE adapters). We asked whether removing a small number of sticky end strands per terminus and only a single distinct sequence might render a terminus inactive; these changes would both increase the sensitivity of the activation process and allow it to be controlled by a single sequence. We compared the nucleation efficiency of termini with seven different patterns of sticky ends strands on their facets (Figure 7b). We found that termini that were missing just the SE sticky end adapter strands (at a total of three sites) nucleated hardly any nanotubes (V5 in Figure 7b), suggesting that this variant could serve as an inactive terminus for activation with just a single SE sticky end strand sequence. These results demonstrate the key design rules for adopting terminus activation as a sensitive nucleic acid diagnostic.

CONCLUSIONS

In this paper, we develop mechanisms to selectively activate and inactivate DNA origami termini for growth of and binding to DNA nanotubes. We design four orthogonal termini that can be distinctly activated and inactivated to dynamically reconfigure doubly terminated nanotube architectures. The terminus activation and inactivation scheme could allow more complex reconfiguration of nanotube networks. For example, selective activation/inactivation of branched termini that nucleate multiple nanotubes[23] could enable the reorganization of specific nanotube geometries. If such nanotube geometries were used to build larger networks, selectively regulating which geometries are active in a network could allow complex morphological changes to be induced. If nanotubes were used as channels or tracks for transportation of molecular cargo, dynamic rearrangement of nanotube connections between termini anchored at different points on a surface or on different objects[26] could be used to regulate when and where signals or materials are transported. Nanotubes could also serve as templates for other materials such as electrically conductive nanoparticles,[41] and self-assembling electrical circuits that could dynamically rewire could be developed. These examples illustrate how selective, molecular scale regulation of nanostructures that direct nanotube network connectivity

https://dx.doi.org/10.1021/acsnano.0c05340
ACS Nano XXXX, XXX, XXX−XXX

could induce structural changes over length scales of 10 μm or more, 1−2 orders of magnitude larger than are induced using most reconfigurable DNA nanostructures.[27−29]

We showed that 50−100 nM activation/inactivation strands, a typical concentration of the strand outputs of many DNA strand displacement cascades and DNA circuits,[27] could be used to control termini. DNA strand displacement circuits could thus control the timed release of DNA signals that regulate different terminus activities to enable autonomous control of desired reconfigurations[42,43] or to only orchestrate a transformation in response to defined chemical patterns.[44] Integrating DNA strand displacement reactions and terminus regulation could allow complex structures to be self-assembled autonomously. For example, autonomously timing the specific activation of different linear and branched termini could give rise to hierarchical structures[1,5] with programmable branch lengths. Activating different arms of multiarmed termini at different times during the growth process could produce anisotropic branched nanotube structures where the length of each nanotube arm was different. Further, as an extension of the results in Figure 6, sequential activation and inactivation of capping termini could act as protection and deprotection steps during the assembly of multidomain nanotubes analogous to block copolymers.[45]

One limitation in our experiments is the lack of continuous nanotube growth in our batch nanotube growth reactions. Growth depletes monomers, causing active nanotube growth to stop after 24 h.[24] Thus, activation of new termini after 24 h likely does not result in new nanotube growth, and the newly activated termini only join to pre-existing nanotubes. We also found that if growth has occurred for 24 h and then a doubly terminated structure is created, removing one of the termini at a later point will likely not result in further nanotube growth. This is in contrast to cellular cytoskeletal filaments whose monomers are maintained at a constant concentration to sustain growth from new structures. A mechanism to sustain nanotube growth will likely be required to fully realize the potential of dynamic and reconfigurable DNA nanotube networks.

We also demonstrated how nanotube activation can be triggered in response to subnanomolar concentrations of a single activation sequence, resulting in the growth of micron-scale structures from nanoscale structures. These results highlight how terminus activation might be improved and adopted as a potentially sensitive isothermal and enzyme-free nucleic acid diagnostic tool. Here, we demonstrated detection of short, 16-base DNA sequences, but longer sequences could be detected as additional overhangs do not influence growth. In our experiments we tracked nanotube assembly with fluorescence, but the individual DNA monomers could be modified with plasmonic nanoparticles such that nanotube assembly triggers an optical change for naked eye detection.[46,47] Other nucleic acid diagnostic tools have taken advantage of such optical changes;[48] however, our approach allows for a simple one-pot assay where amplification is achieved through control over nucleation and no sample manipulation is required after the input is added. Our approach also allows for easy multiplexing as multiple orthogonal termini can be designed and operated together in a single solution. Additionally, through the use of DNA strand displacement translator circuits or aptaswitches,[49,50] terminus activation could be adapted to detect a wide range of biochemicals.

Terminus inactivation might also potentially be used for the triggered release of therapeutics.[20,51] For example, if doubly terminated nanotubes were loaded with therapeutic molecules, removal of termini from nanotube ends in response to specific disease markers could trigger drug release. As nanotubes can grow to tens of microns in length, doubly terminated structures could potentially encapsulate a lot of cargo and only require picomolar concentrations of stimulus for release.

MATERIALS AND METHODS

DNA Components. All oligonucleotides used in this study were synthesized by Integrated DNA Technologies (IDT). The sequences of the DNA monomers are in Supporting Information Section 1.1. M13mp18 DNA (7240 bases) was purchased from Bayou Biolabs (cat. no. P-107). The sequences of the staple strands, adapter strands, and activation/inactivation strands of the DNA origami termini are in Supporting Information Sections 1.3 and 1.4. The labeling strands for the DNA origami termini have the same structure and sequence as those used in previous works[24] (Supporting Information Section 1.5).

Preparation of DNA Monomer Mixtures and DNA Origami Termini. DNA origami termini were annealed in an Eppendorf Mastercycler in 40 mM Tris-acetate, 1 mM EDTA buffer supplemented with 12.5 mM magnesium acetate (TAEM) following previously reported methods.[14,26] A DNA origami terminus is composed of a scaffold strand (M13mp18 DNA), 24 staple strands, and 18 adapter strands. Termini were fluorescently labeled using a mixture of labeling strands that bind to unfolded M13 DNA and provide a docking site for a fluorescently labeled strand (100 labeling sites per terminus)[24,26] (Supporting Information Section 1.2). For fluorescent tags used in each experiment, see Supporting Information Table S21. Inactive DNA origami termini were annealed in TAEM buffer with 5 nM M13 DNA, 500 nM of each staple strand, 100 nM of each adapter strand, 10 nM of each labeling strand, and 1000 nM of the fluorescently labeled strand. Termini annealed in an active state also included each activation strand at 600 nM. Biotinylated-BSA at a final concentration of 0.05 mg/mL (cat. no. A8549, Sigma-Aldrich) was also included to prevent termini from sticking to the walls of the annealing tubes.[26] Annealing was conducted as follows: samples were incubated at 90 °C for 5 min, cooled from 90 to 45 °C at 1 °C/min, held at 45 °C for 1 h, and then cooled from 45 to 20 °C at 0.1 °C/min. After annealing, termini were purified with a centrifugal filter (100 kDa Amico Ultra-0.5 mL, cat. no. UFC510096) to remove excess staple, adapter, and labeling strands. For purification, 50 μL of the annealed terminus mixture and 350 μL of TAEM buffer were added to the filter and centrifuged at 2000 RCF for 4 min. The samples were washed three more times by adding 200 μL of TAEM buffer to the remain solution and repeating centrifugation. The final sample was eluted by inverting the filter into a fresh tube and centrifuging briefly. Purified termini were stored at room temperature until used. Typically, termini were annealed the day before they were used.

Terminus Activation and Inactivation Experiments. To test terminus activation and inactivation, DNA monomer strands were freshly annealed in an Eppendorf Mastercycler in TAEM. Monomer mixes contained 90 nM of the RE and SE monomer sticky end strands (strands 2 and 4 in Supporting Information Section 1.1) and 45 nM of the other RE and SE strands (strands 1, 3, and 5 in Supporting Information Section 1.1). Biotinylated-BSA at a final concentration of 0.05 mg/mL (cat. no. A8549, Sigma-Aldrich) was also included to prevent monomers from sticking to the walls of the annealing tubes.[26] Slight differences between stocks of monomer mixes and BSA solutions and variations in pipetted volumes during sample preparation and imaging introduced variation in the observed fractions of nanotubes with termini and termini with nanotubes from experiment-to-experiment. For each experimental sample, enough monomer mix was prepared to split into aliquots for each experimental time point prior to annealing. To anneal the monomers, samples were initially held at 90 °C for 5 min, cooled to 20 °C at −1 °C/min, and subsequently held at 20 °C for the duration of the

https://dx.doi.org/10.1021/acsnano.0c05340
ACS Nano XXXX, XXX, XXX−XXX

experiment. As soon as the samples reached 20 °C, the appropriate DNA origami termini were added to all of the aliquots to begin the experiment. DNA origami termini were typically added to a final concentration of 5−10 pM (see Supporting Information Table S22 for exact termini concentrations for each experiment). Thus, the state of a reaction at each time point in a given experiment was measured using a reaction in its own PCR tube; this methodology could introduce variation between time point to time point of an order that might be expected from experiment to experiment. After an initial incubation period followed by fluorescence imaging, the appropriate DNA activation or inactivation strands were added to all of the aliquots, and the appropriate time point aliquot was imaged after another incubation period. Unless otherwise noted, activation strands were added to a final concentration of 50 nM, and inactivation strands were added to a final concentration of 100 nM. The lengths of the incubation periods varied between experiments and are tabulated in Supporting Information Section 2.1.

Stepwise Hierarchical Structure Assembly Experiments. To test stepwise assembly of branched nanotube structures *via* seed inactivation and end-to-end joining, we prepared A1 and B1 termini using the methods described above and prepared Y-shaped DNA origami termini using methods described in ref 23. Nanotubes were grown from A1 termini with 55 nM of monomers and from Y termini with 130 nM monomers. All termini were added to a final concentration of 5 pm. Nanotube growth from A1 and Y termini was conducted separately for 20 h at 20 °C. Active B1 termini were then added to the A1 terminated nanotubes after and incubated for an additional 13 h to allow the caps to attach. A1−B1 doubly terminated nanotubes were then mixed with Y nanotube structures at a ratio of 12:1 to ensure excess A1−B1 terminated structures were present for end-to-end joining. The A1 inactivation strand was then added to a final concentration of 100 nM, and the mixture was incubated at 20 °C for an additional 48 h to allow for A1 inactivation and subsequent end-to-end joining.

Fluorescence Imaging and Analysis. Fluorescence imaging was conducted on an inverted microscope (Olympus IX71) using a 60×/1.45 NA oil immersion objective with 1.6× magnification. Images were captured on a cooled CCD camera (iXon3, Andor). For fluorescence imaging, 1 μL was taken from the appropriate time point aliquot and diluted 6-fold in TAEM containing 100 nM preannealed, nonfluorescent RE monomers without sticky end strands to reduce background fluorescence from unincorporated monomers. After dilution, 6 μL of prepared sample was added to an 18 mm × 18 mm glass coverslip (cat. no. 48366 045, VWR) that was then inverted onto a glass slide (cat. no. 16004−424, VWR). Images were then captured at 3−5 randomly selected locations. All fluorescence images were processed and analyzed using custom MATLAB scripts (Supporting Information Section 6).

ASSOCIATED CONTENT

Supporting Information

The Supporting Information is available free of charge at https://pubs.acs.org/doi/10.1021/acsnano.0c05340.

All DNA sequence information, additional experiments and experimental methods, and image analysis protocols (PDF)

AUTHOR INFORMATION

Corresponding Author

Rebecca Schulman − *Chemical and Biomolecular Engineering, Computer Science, and Chemistry, Johns Hopkins University, Baltimore, Maryland 21218, United States;* orcid.org/0000-0003-4555-3162; Email: rschulm3@jhu.edu

Authors

Samuel W. Schaffter − *Chemical and Biomolecular Engineering, Johns Hopkins University, Baltimore, Maryland 21218, United States*

Joanna Schneider − *Chemical and Biomolecular Engineering, Johns Hopkins University, Baltimore, Maryland 21218, United States*

Deepak K. Agrawal − *Chemical and Biomolecular Engineering, Johns Hopkins University, Baltimore, Maryland 21218, United States*

Michael S. Pacella − *Chemical and Biomolecular Engineering, Johns Hopkins University, Baltimore, Maryland 21218, United States;* orcid.org/0000-0001-8919-147X

Eric Rothchild − *Material Science and Engineering, Johns Hopkins University, Baltimore, Maryland 21218, United States*

Terence Murphy − *Our Lady of Lourdes High School, Poughkeepsie, New York 12603, United States*

Complete contact information is available at: https://pubs.acs.org/10.1021/acsnano.0c05340

Author Contributions

#S.W.S. and J.S. contributed equally to this work. S.W.S., J.S., D.A., M.P., and R.S. conceived and designed research. J.S. conducted most experiments. S.W.S. and J.S. conducted most data analysis. D.A., M.P., E.R., and T.M. conducted supporting experiments. S.W.S. and R.S. wrote the paper with input from all other authors.

Notes

The authors declare no competing financial interest.

ACKNOWLEDGMENTS

The authors thank J. Fern and S. Jia for insightful conversations. This material is based upon work supported by the National Science Foundation Graduate Research Fellowship under grant no. DGE-1232825. This work was supported by the Department of Energy under grant no. DE-SC001 0426 for materials and supply costs.

REFERENCES

(1) Fletcher, D. A.; Mullins, R. D. Cell Mechanics and the Cytoskeleton. *Nature* **2010**, *463*, 485−492.

(2) Petry, S.; Vale, R. D. Microtubule Nucleation at the Centrosome and Beyond. *Nat. Cell Biol.* **2015**, *17*, 1089−1093.

(3) Blanchoin, L.; Boujemaa-Paterski, R.; Sykes, C.; Plastino, J. Actin Dynamics, Architecture, and Mechanics in Cell Motility. *Physiol. Rev.* **2014**, *94*, 235−263.

(4) Basnet, N.; Nedozralova, H.; Crevenna, A. H.; Bodakuntla, S.; Schlichthaerle, T.; Taschner, M.; Cardone, G.; Janke, C.; Jungmann, R.; Magiera, M. M.; Biertümpfel, C.; Mizuno, N. Direct Induction of Microtubule Branching by Microtubule Nucleation Factor SSNA1. *Nat. Cell Biol.* **2018**, *20*, 1172−1180.

(5) Kapitein, L. C.; Hoogenraad, C. C. Building the Neuronal Microtubule Cytoskeleton. *Neuron* **2015**, *87*, 492−506.

(6) Bailey, C. H.; Kandel, E. R. Chapter 10 Synaptic Remodeling, Synaptic Growth and the Storage of Long-Term Memory in Aplysia. In *Progress in Brain Research*; Sossin, W. S., Lacaille, J.-C., Castellucci, V. F., Belleville, S., Eds.; Elsevier: Amsterdam, Netherlands, 2008; Vol. *169*, pp 179−198.

(7) Maune, H. T.; Han, S.; Barish, R. D.; Bockrath, M.; Goddard, W. A., III; Rothemund, P. W. K.; Winfree, E. Self-Assembly of Carbon Nanotubes into Two-Dimensional Geometries Using DNA Origami Templates. *Nat. Nanotechnol.* **2010**, *5*, 61−66.

(8) Sanchez-Valencia, J. R.; Dienel, T.; Gröning, O.; Shorubalko, I.; Mueller, A.; Jansen, M.; Amsharov, K.; Ruffieux, P.; Fasel, R.

Controlled Synthesis of Single-Chirality Carbon Nanotubes. *Nature* **2014**, *512*, 61.
(9) Serra, M.; Arenal, R.; Tenne, R. An Overview of the Recent Advances in Inorganic Nanotubes. *Nanoscale* **2019**, *11*, 8073−8090.
(10) Shen, H.; Fallas, J. A.; Lynch, E.; Sheffler, W.; Parry, B.; Jannetty, N.; Decarreau, J.; Wagenbach, M.; Vicente, J. J.; Chen, J.; Wang, L.; Dowling, Q.; Oberdorfer, G.; Stewart, L.; Wordeman, L.; De Yoreo, J.; Jacobs-Wagner, C.; Kollman, J.; Baker, D. De Novo Design of Self-Assembling Helical Protein Filaments. *Science* **2018**, *362*, 705−709.
(11) Nishinaka, T.; Takano, A.; Doi, Y.; Hashimoto, M.; Nakamura, A.; Matsushita, Y.; Kumaki, J.; Yashima, E. Conductive Metal Nanowires Templated by the Nucleoprotein Filaments, Complex of DNA and RecA Protein. *J. Am. Chem. Soc.* **2005**, *127*, 8120−8125.
(12) Brodin, J. D.; Smith, S. J.; Carr, J. R.; Tezcan, F. A. Designed, Helical Protein Nanotubes with Variable Diameters from a Single Building Block. *J. Am. Chem. Soc.* **2015**, *137*, 10468−10471.
(13) Rothemund, P. W. K.; Ekani-Nkodo, A.; Papadakis, N.; Kumar, A.; Fygenson, D. K.; Winfree, E. Design and Characterization of Programmable DNA Nanotubes. *J. Am. Chem. Soc.* **2004**, *126*, 16344−16352.
(14) Mohammed, A. M.; Schulman, R. Directing Self-Assembly of DNA Nanotubes Using Programmable Seeds. *Nano Lett.* **2013**, *13*, 4006−4013.
(15) Liu, D.; Park, S. H.; Reif, J. H.; LaBean, T. H. DNA Nanotubes Self-Assembled from Triple-Crossover Tiles as Templates for Conductive Nanowires. *Proc. Natl. Acad. Sci. U. S. A.* **2004**, *101*, 717−722.
(16) Han, D.; Pal, S.; Nangreave, J.; Deng, Z.; Liu, Y.; Yan, H. DNA Origami with Complex Curvatures in Three-Dimensional Space. *Science* **2011**, *332*, 342−346.
(17) Rothemund, P. W. K. Folding DNA to Create Nanoscale Shapes and Patterns. *Nature* **2006**, *440*, 297−302.
(18) Wei, B.; Dai, M.; Yin, P. Complex Shapes Self-Assembled from Single-Stranded DNA Tiles. *Nature* **2012**, *485*, 623−626.
(19) Ke, Y.; Ong, L. L.; Shih, W. M.; Yin, P. Three-Dimensional Structures Self-Assembled from DNA Bricks. *Science* **2012**, *338*, 1177.
(20) Lo, P. K.; Karam, P.; Aldaye, F. A.; McLaughlin, C. K.; Hamblin, G. D.; Cosa, G.; Sleiman, H. F. Loading and Selective Release of Cargo in DNA Nanotubes with Longitudinal Variation. *Nat. Chem.* **2010**, *2*, 319−328.
(21) Wilner, O. I.; Orbach, R.; Henning, A.; Teller, C.; Yehezkeli, O.; Mertig, M.; Harries, D.; Willner, I. Self-Assembly of DNA Nanotubes with Controllable Diameters. *Nat. Commun.* **2011**, *2*, 540.
(22) Yin, P.; Hariadi, R. F.; Sahu, S.; Choi, H. M. T.; Park, S. H.; LaBean, T. H.; Reif, J. H. Programming DNA Tube Circumferences. *Science* **2008**, *321*, 824−826.
(23) Jorgenson, T. D.; Mohammed, A. M.; Agrawal, D. K.; Schulman, R. Self-Assembly of Hierarchical DNA Nanotube Architectures with Well-Defined Geometries. *ACS Nano* **2017**, *11*, 1927−1936.
(24) Agrawal, D. K.; Jiang, R.; Reinhart, S.; Mohammed, A. M.; Jorgenson, T. D.; Schulman, R. Terminating DNA Tile Assembly with Nanostructured Caps. *ACS Nano* **2017**, *11*, 9770−9779.
(25) Mohammed, A. M.; Velazquez, L.; Chisenhall, A.; Schiffels, D.; Fygenson, D. K.; Schulman, R. Self-Assembly of Precisely Defined DNA Nanotube Superstructures Using DNA Origami Seeds. *Nanoscale* **2017**, *9*, 522−526.
(26) Mohammed, A. M.; Šulc, P.; Zenk, J.; Schulman, R. Self-Assembling DNA Nanotubes to Connect Molecular Landmarks. *Nat. Nanotechnol.* **2017**, *12*, 312−316.
(27) Zhang, D. Y.; Seelig, G. Dynamic DNA Nanotechnology Using Strand-Displacement Reactions. *Nat. Chem.* **2011**, *3*, 103−113.
(28) Wang, M.; Dong, J.; Zhou, C.; Xie, H.; Ni, W.; Wang, S.; Jin, H.; Wang, Q. Reconfigurable Plasmonic Diastereomers Assembled by DNA Origami. *ACS Nano* **2019**, *13*, 13702−13708.
(29) Petersen, P.; Tikhomirov, G.; Qian, L. Information-Based Autonomous Reconfiguration in Systems of Interacting DNA Nanostructures. *Nat. Commun.* **2018**, *9*, 5362.
(30) Pearson, A. C.; Liu, J.; Pound, E.; Uprety, B.; Woolley, A. T.; Davis, R. C.; Harb, J. N. DNA Origami Metallized Site Specifically to Form Electrically Conductive Nanowires. *J. Phys. Chem. B* **2012**, *116*, 10551−10560.
(31) Kuzyk, A.; Schreiber, R.; Fan, Z.; Pardatscher, G.; Roller, E.-M.; Högele, A.; Simmel, F. C.; Govorov, A. O.; Liedl, T. DNA-Based Self-Assembly of Chiral Plasmonic Nanostructures with Tailored Optical Response. *Nature* **2012**, *483*, 311−314.
(32) Bui, H.; Onodera, C.; Kidwell, C.; Tan, Y.; Graugnard, E.; Kuang, W.; Lee, J.; Knowlton, W. B.; Yurke, B.; Hughes, W. L. Programmable Periodicity of Quantum Dot Arrays with DNA Origami Nanotubes. *Nano Lett.* **2010**, *10*, 3367−3372.
(33) Chandrasekaran, A. R. Programmable DNA Scaffolds for Spatially-Ordered Protein Assembly. *Nanoscale* **2016**, *8*, 4436−4446.
(34) Sharma, J.; Chhabra, R.; Cheng, A.; Brownell, J.; Liu, Y.; Yan, H. Control of Self-Assembly of DNA Tubules Through Integration of Gold Nanoparticles. *Science* **2009**, *323*, 112−116.
(35) Fu, T. J.; Seeman, N. C. DNA Double-Crossover Molecules. *Biochemistry* **1993**, *32*, 3211−3220.
(36) Zhang, D. Y.; Winfree, E. Control of DNA Strand Displacement Kinetics Using Toehold Exchange. *J. Am. Chem. Soc.* **2009**, *131*, 17303−17314.
(37) Ekani-Nkodo, A.; Kumar, A.; Fygenson, D. K. Joining and Scission in the Self-Assembly of Nanotubes from DNA Tiles. *Phys. Rev. Lett.* **2004**, *93*, 268301.
(38) Zhang, D. Y.; Hariadi, R. F.; Choi, H. M. T.; Winfree, E. Integrating DNA Strand-Displacement Circuitry with DNA Tile Self-Assembly. *Nat. Commun.* **2013**, *4*, 1965.
(39) Ranallo, S.; Sorrentino, D.; Ricci, F. Orthogonal Regulation of DNA Nanostructure Self-Assembly and Disassembly Using Antibodies. *Nat. Commun.* **2019**, *10*, 5509.
(40) Minev, D.; Wintersinger, C. M.; Ershova, A.; Shih, W. M. *Robust Nucleation Control via Crisscross Polymerization of DNA Slats*. 2019. bioRxiv. DOI: 10.1101/2019.12.11.873349 (accessed May 15, 2020).
(41) Gates, E. P.; Jensen, J. K.; Harb, J. N.; Woolley, A. T. Optimizing Gold Nanoparticle Seeding Density on DNA Origami. *RSC Adv.* **2015**, *5*, 8134−8141.
(42) Fern, J.; Scalise, D.; Cangialosi, A.; Howie, D.; Potters, L.; Schulman, R. DNA Strand-Displacement Timer Circuits. *ACS Synth. Biol.* **2017**, *6*, 190−193.
(43) Scalise, D.; Rubanov, M.; Miller, K.; Potters, L.; Noble, M.; Schulman, R. Programming the Sequential Release of DNA. *ACS Synth. Biol.* **2020**, *9*, 749−755.
(44) Cherry, K. M.; Qian, L. Scaling up Molecular Pattern Recognition with DNA-Based Winner-Take-All Neural Networks. *Nature* **2018**, *559*, 370−376.
(45) Mai, Y.; Eisenberg, A. Self-Assembly of Block Copolymers. *Chem. Soc. Rev.* **2012**, *41*, 5969−5985.
(46) Yu, T.; Wei, Q. Plasmonic Molecular Assays: Recent Advances and Applications for Mobile Health. *Nano Res.* **2018**, *11*, 5439−5473.
(47) Tan, S. J.; Campolongo, M. J.; Luo, D.; Cheng, W. Building Plasmonic Nanostructures with DNA. *Nat. Nanotechnol.* **2011**, *6*, 268−276.
(48) Taton, T. A.; Mirkin, C. A.; Letsinger, R. L. Scanometric DNA Array Detection with Nanoparticle Probes. *Science* **2000**, *289*, 1757.
(49) Fern, J.; Schulman, R. Modular DNA Strand-Displacement Controllers for Directing Material Expansion. *Nat. Commun.* **2018**, *9*, 3766.
(50) Seelig, G.; Soloveichik, D.; Zhang, D. Y.; Winfree, E. Enzyme-Free Nucleic Acid Logic Circuits. *Science* **2006**, *314*, 1585−1588.
(51) Sellner, S.; Kocabey, S.; Nekolla, K.; Krombach, F.; Liedl, T.; Rehberg, M. DNA Nanotubes as Intracellular Delivery Vehicles *in Vivo*. *Biomaterials* **2015**, *53*, 453−463.

https://dx.doi.org/10.1021/acsnano.0c05340
ACS Nano XXXX, XXX, XXX−XXX